Some aspects of seismic anisotropy

Elasticity tensor and symmetries of the medium

For seismic anisotropy we start with the general relation between stress and strain according to Hooke:

$$\sigma_{ij} = c_{ijkl}\epsilon_{kl}$$

where σ_{ij} is the stress tensor, ϵ_{kl} the strain tensor, and c_{ijkl} is the elasticity (or stiffness) tensor. This 4th order tensor has $3^4 = 81$ elements of which only 21 are independent ($c_{ijkl} = c_{jikl} = c_{ijlk} = c_{klij}$).

The 21 coefficients for an arbitrary isotropic medium are often arranged in a 6x6 matrix, the stiffness matrix C_{ij}

$$C = \begin{pmatrix} c_{1111} & c_{1122} & c_{1133} & c_{1123} & c_{1113} & c_{1112} \\ c_{2211} & c_{2222} & c_{2233} & c_{2223} & c_{2213} & c_{2212} \\ c_{3311} & c_{3322} & c_{3333} & c_{3323} & c_{3313} & c_{3312} \\ c_{2311} & c_{2322} & c_{2333} & c_{2323} & c_{2313} & c_{2312} \\ c_{1311} & c_{1322} & c_{1333} & c_{1323} & c_{1313} & c_{1312} \\ c_{1211} & c_{1222} & c_{1233} & c_{1223} & c_{1213} & c_{1212} \end{pmatrix}$$

[Pairs (i, j) or (k, l) of the elasticity tensor convert to indices of C_{ij} according to: $(1, 1) \rightarrow 1$, $(2, 2) \rightarrow 2$, $(3, 3) \rightarrow 3$, $(2, 3) \rightarrow 4$, $(1, 3) \rightarrow 5$, $(1, 2) \rightarrow 6$.]

There are many minerals in crust, mantle and core that have anisotropic properties. How many independent coefficients the elasticity tensor of each of the crystals has, depends on the crystallographic structure. A medium with hexagonal symmetry has 5 independent coefficients. Hexagonal symmetry, or, equivalently, cylindrical symmetry, is of particular interest to seismology because it is relatively simple and it can approximate many actual situations in the Earth (e.g. alignment of olivine crystals along the $\vec{a}$ axis with randomly oriented $\vec{b}$ and $\vec{c}$ axes, or laminated structure).
A medium with hexagonal symmetry with a vertical symmetry axis is called transversely isotropic. A medium with hexagonal symmetry with a horizontal symmetry axis is called azimuthally anisotropic.

Wave propagation in anisotropic media

Seismic anisotropy distorts the particle motion and, in general, no clear distinction can be made between the modes of elastic waves such as P and S waves in the isotropic case. This implies seismic velocity variations as a function of (1) propagation direction and (2) polarization direction of the seismic waves. This will be shown from the solutions of the wave equation in an anisotropic medium. Assume a homogeneous anisotropic medium and a plane wave solution with phase velocity c, amplitude and polarization vector $\vec{a}$, and propagation direction $\vec{n}$:

$$\vec{u}(\vec{r}, t) = \vec{a} f(t - \frac{\vec{n} \cdot \vec{r}}{c})$$

Our problem is now to find suitable combinations of c and $\vec{a}$ that satisfy the anisotropic wave equation for a wave travelling in the $\vec{n}$ direction:

$$c_{ijkl}\partial_j\partial_k u_l = \rho\partial_{tt} u_i$$

Substitution of the plane wave solution $\vec{u}$ in the wave equation:

$$c_{ijkl}\partial_j\partial_k[a_l f(t - \frac{\vec{n} \cdot \vec{r}}{c})] = \rho\partial_{tt}[a_i f(t - \frac{\vec{n} \cdot \vec{r}}{c})]$$

gives

$$c_{ijkl}a_l n_j n_k \frac{1}{c^2} = \rho a_i$$

or

$$m_{il}a_l = c^2 a_i$$

with

$$m_{il} = \frac{1}{\rho} c_{ijkl} n_j n_k$$

The matrix M is called the Christoffel matrix. If we find the eigenvalues and eigenvectors of the matrix m_{il}, we have the phase velocities and the propagation directions of the independent wave types. This will be illustrated in the following for isotropic and hexagonal media.

Type of symmetry	**Number of independent elastic coefficients**	**Typical mineral**
isotropic solid	2	volcanic glass
cubic	3	garnet
hexagonal	5	ice
trigonal I	7	ilmenite
trigonal II	6	quartz
tetragonal	6	stishovite
orthorhombic	9	olivine
monoclinic	13	hornblende
triclinic	21	plagioclase

Table 1: Number of independent elastic coefficients for selected symmetry systems and typical minerals or Earth's materials

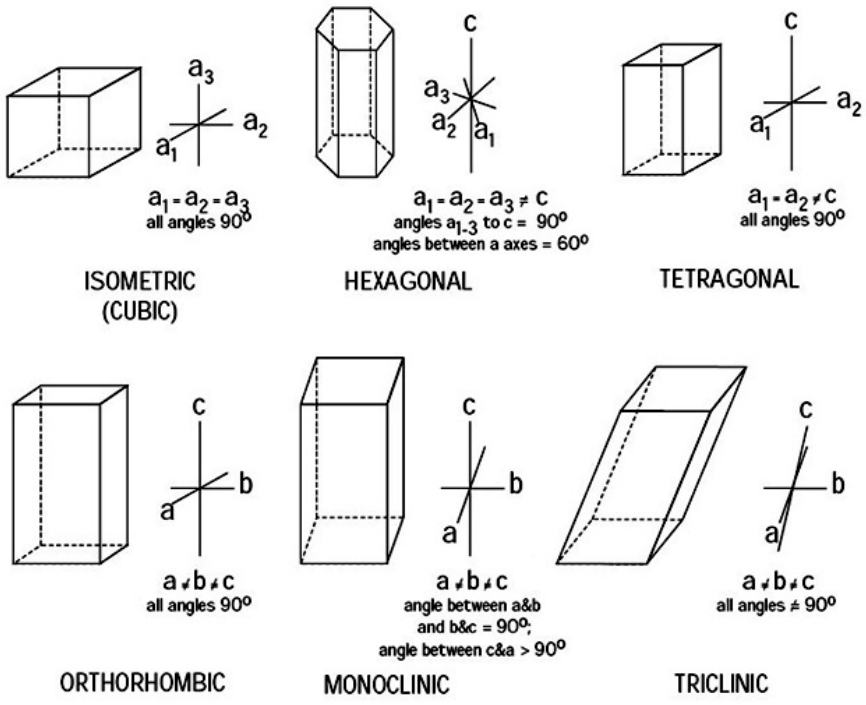

Figure 1: Examples of symmetry planes in the different symmetry systems.

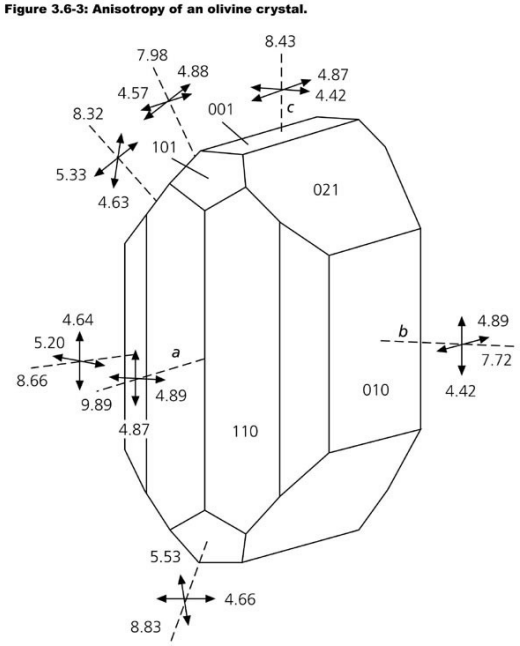

Figure 2: Compressional and shear-wave velocities in a momocrystal of olivine. Original data from Kumazawa & Anderson (1969).

Isotropic medium

First we solve the system for an isotropic medium

$$m_{il} = \frac{1}{\rho} c_{ijkl} n_j n_k$$

with

$$c_{ijkl} = \lambda \delta_{ij} \delta_{kl} + \mu(\delta_{ik}\delta_{jl} + \delta_{il}\delta_{jk})$$

Using $\vec{n} = (n_1, n_2, n_3)^T$ with $n_1^2 + n_2^2 + n_3^2 = 1$:

$$m_{il} = \frac{1}{\rho}[\lambda \delta_{ij} \delta_{kl} + \mu(\delta_{ik}\delta_{jl} + \delta_{il}\delta_{jk})] n_j n_k$$

we find

$$m_{il} = \frac{1}{\rho}[\lambda n_i n_l + \mu(n_i n_l + \delta_{il}(n_1 n_1 + n_2 n_2 + n_3 n_3))]$$

$$m_{il} = \frac{1}{\rho}[\lambda n_i n_l + \mu(n_i n_l + \delta_{il})]$$

Thus

$$M = \frac{1}{\rho} \begin{pmatrix} (\lambda+\mu)n_1^2 + \mu & (\lambda+\mu)n_1 n_2 & (\lambda+\mu)n_1 n_3 \\ (\lambda+\mu)n_1 n_2 & (\lambda+\mu)n_2^2 + \mu & (\lambda+\mu)n_2 n_3 \\ (\lambda+\mu)n_1 n_3 & (\lambda+\mu)n_2 n_3 & (\lambda+\mu)n_3^2 + \mu \end{pmatrix}$$

The eigenvalues are obtained from $\det(M - \Lambda I) = 0$, giving $\frac{1}{\rho^3}(\mu - \Lambda)^2(\lambda + 2\mu - \Lambda) = 0$ where Λ denotes the eigenvalue. We find the eigenvalues $\Lambda_1 = \Lambda_2 = \frac{\mu}{\rho}$ and $\Lambda_3 = \frac{\lambda+2\mu}{\rho}$. Checking the expression of the Christoffel matrix $m_{il}a_l = c^2 \rho a_i$ we find that the eigenvalues are related to the phase velocities: $c_1 = \sqrt{\frac{\mu}{\rho}}$, $c_2 = \sqrt{\frac{\mu}{\rho}}$, and $c_3 = \sqrt{\frac{\lambda+2\mu}{\rho}}$.
The eigenvectors $\vec{a}$ corresponding to the first two eigenvalues Λ_1 and Λ_2 are found to satisfy $n_1 a_1 + n_2 a_2 + n_3 a_3 = 0$. This means that the two orthogonal eigenvectors are perpendicular to the propagation direction $\vec{n}$. The eigenvector corresponding to Λ_3 satisfies $\vec{a} = \vec{n}$. Thus we have found

3 independent plane wave solutions of the isotropic wave equation: one P-wave and two S-waves. The phase velocities are obtained from the eigenvalues of the Christoffel matrix, the polarizations are determined by the eigenvectors.

Note that the stiffness matrix C_{ij} for the isotropic case is:

$$C = \begin{pmatrix} \lambda+2\mu & \lambda & \lambda & 0 & 0 & 0 \\ \lambda & \lambda+2\mu & \lambda & 0 & 0 & 0 \\ \lambda & \lambda & \lambda+2\mu & 0 & 0 & 0 \\ 0 & 0 & 0 & \mu & 0 & 0 \\ 0 & 0 & 0 & 0 & \mu & 0 \\ 0 & 0 & 0 & 0 & 0 & \mu \end{pmatrix}$$

Hexagonal symmetry

For hexagonal symmetry with a vertical (x_3) symmetry axis (transverse isotropy) the stiffness matrix is:

$$C = \begin{pmatrix} A & A-2N & F & 0 & 0 & 0 \\ A-2N & A & F & 0 & 0 & 0 \\ F & F & C & 0 & 0 & 0 \\ 0 & 0 & 0 & L & 0 & 0 \\ 0 & 0 & 0 & 0 & L & 0 \\ 0 & 0 & 0 & 0 & 0 & N \end{pmatrix}$$

with the coefficients A, C, F, L, and N according to Love (1927).
If we choose

$$\vec{n} = \begin{pmatrix} 1 \\ 0 \\ 0 \end{pmatrix}$$

we obtain

$$m_{il} = \frac{1}{\rho} c_{ijkl} n_j n_k = \frac{1}{\rho} c_{i11l}$$

or

$$M = \begin{pmatrix} m_{11} & m_{12} & m_{13} \\ m_{21} & m_{22} & m_{23} \\ m_{31} & m_{32} & m_{33} \end{pmatrix} = \frac{1}{\rho} \begin{pmatrix} c_{1111} & c_{1112} & c_{1113} \\ c_{2111} & c_{2112} & c_{2113} \\ c_{3111} & c_{3112} & c_{3113} \end{pmatrix} = \frac{1}{\rho} \begin{pmatrix} C_{11} & C_{16} & C_{15} \\ C_{61} & C_{66} & C_{65} \\ C_{51} & C_{56} & C_{55} \end{pmatrix}$$

or

$$M = \frac{1}{\rho} \begin{pmatrix} A & 0 & 0 \\ 0 & N & 0 \\ 0 & 0 & L \end{pmatrix}$$

We immediately recognize the eigenvalues:

$$\begin{aligned} \lambda_1 &= \tfrac{A}{\rho} \\ \lambda_2 &= \tfrac{N}{\rho} \\ \lambda_3 &= \tfrac{L}{\rho} \end{aligned}$$

and find the corresponding phase velocities:

$$\begin{aligned} c_1 &= \sqrt{\tfrac{A}{\rho}} \quad `P' \\ c_2 &= \sqrt{\tfrac{N}{\rho}} \quad `S' \\ c_3 &= \sqrt{\tfrac{L}{\rho}} \quad `S' \end{aligned}$$

with the polarization vecors:

$$\vec{a}_1 = \begin{pmatrix} 1 \\ 0 \\ 0 \end{pmatrix}$$
$$\vec{a}_2 = \begin{pmatrix} 0 \\ 1 \\ 0 \end{pmatrix}$$
$$\vec{a}_3 = \begin{pmatrix} 0 \\ 0 \\ 1 \end{pmatrix}$$

This means that for propagation along the x_1 axis (in a medium with hexagonal symmetry with a vertical symmetry axis such as a layered medium), we have 3 waves with different velocity and polarization, one of P-type with phase velocity $\alpha_H = \sqrt{\frac{A}{\rho}}$, and two of S-type. If an S-wave enters the medium along the x_1 axis with components of polarization along both the x_2 and x_3 axes, the two components along these axes will propagate at different speeds. This is called shear-wave splitting.

Figure 3.6-2: The effects of transverse isotropy due to layering.

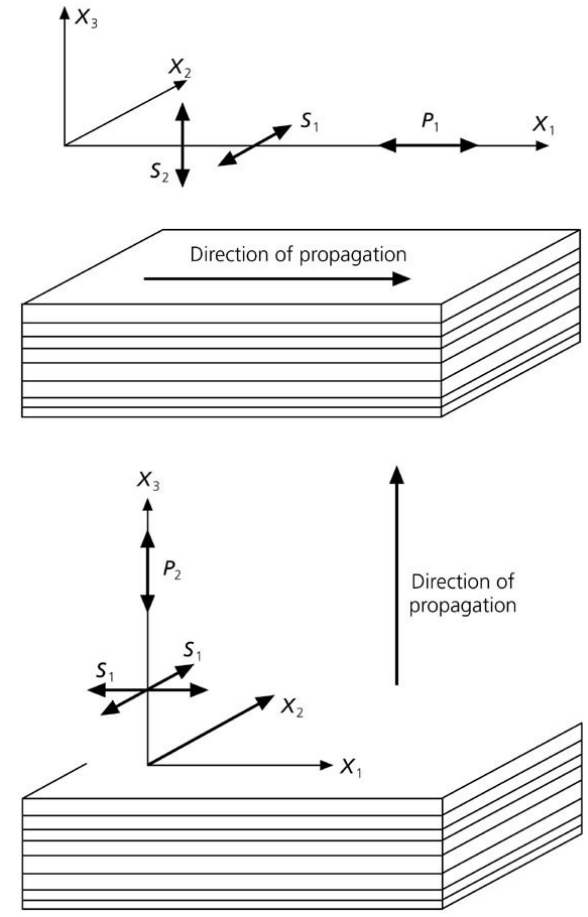

Figure 3: (Top) Three possible seismic plane-waves propagating in the plane perpendicular to the symmetry axis (x_3 here). (Bottom) P and S waves propagating in the direction of the symmetry axis.

Now we choose

$$\vec{n} = \begin{pmatrix} 0 \\ 0 \\ 1 \end{pmatrix}$$

for vertically propagating waves. We obtain

$$m_{il} = \frac{1}{\rho} c_{ijkl} n_j n_k = \frac{1}{\rho} c_{i33l} = \frac{1}{\rho} \begin{pmatrix} L & 0 & 0 \\ 0 & L & 0 \\ 0 & 0 & C \end{pmatrix}$$

and find waves with

$$\begin{array}{lll} \lambda_1 = \frac{L}{\rho} & c_1 = \sqrt{\frac{L}{\rho}} & `S' \\ \lambda_2 = \frac{L}{\rho} & c_2 = \sqrt{\frac{L}{\rho}} & `S' \\ \lambda_3 = \frac{C}{\rho} & c_3 = \sqrt{\frac{C}{\rho}} & `P' \end{array}$$

with polarization vectors

$$\vec{a}_1 = \begin{pmatrix} 1 \\ 0 \\ 0 \end{pmatrix} \quad \vec{a}_2 = \begin{pmatrix} 0 \\ 1 \\ 0 \end{pmatrix} \quad \vec{a}_3 = \begin{pmatrix} 0 \\ 0 \\ 1 \end{pmatrix}$$

The first two solutions are of S-type (polarization $\perp$ propagation). Note that there is no shear wave splitting for propagation in the x_3 direction. However, we see that the P-wave in the x_1 direction travels with a different speed than the one in the x_3 direction.
For a stack of isotropic layers, one can show that $A > C$ and $N > L$, so that $\alpha_H > \alpha_V$ and $\beta_H > \beta_V$. For intermediate directions the polarization vector $\vec{a}$ is not necessarily parallel (or perpendicular) to the propagation direction $\vec{n}$.

Phase and group velocity

The fact that the phase velocity varies with the direction of propagation leads to a further complication which does not exist in isotropic media. The direction of propagation of the energy of a wave packet may be different from the direction $\vec{n}$ of propagation of the phase. The group-velocity vector $\vec{v}$ does not coincide with the phase-velocity vector $\vec{c}$ except for particular directions. Consider a plane wave propagating in an anisotropic medium and a screen with a large slot parallel to the plane wave as shown in the figure. If Huygens principle is used to propagate the plane wave from the elementary point sources in the slot, we obtain non-circular wavefronts due to directional dependent phase velocities, and see that constructive interference may take place in an obliques direction with regard to the normal $\vec{n}$ of the incident plane wave. For weak anisotropy the departure of the group-velcity vector from the normal $\vec{n}$ remains quite small.

Weak anisotropy

In general, if a P or S wave is incident on an anisotropic structure, three mutually orthogonal waves are excited which travel at different speeds. However, when the anisotropy is weak, the nature of anisotropy can be described as perturbations to the isotropic situation. We then speak of quasi P- and S-waves: qP and qS. For weak anisotropy one finds (Backus, 1965; Crampin, 1977):

$$\rho V_P^2 = A + B_c \cos 2\theta + B_s \sin 2\theta + C_c \cos 4\theta + C_s \sin 4\theta$$

$$\rho V_{SH}^2 = D + E_c \cos 4\theta + E_s \sin 4\theta$$

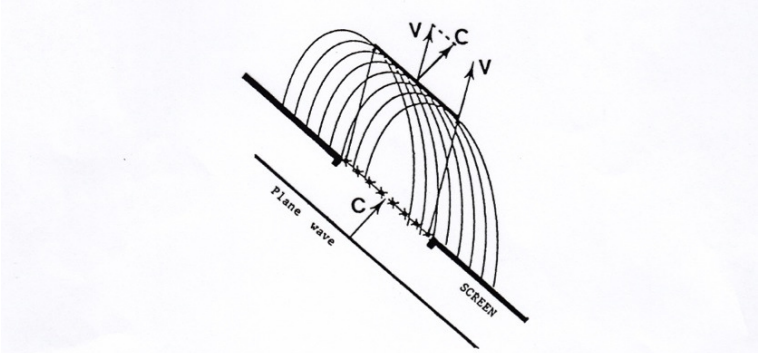

Figure 2-5 Illustration of the concept of group velocity v and phase velocity c in anisotropic media (modified from Garmany, 1989). The phase velocity vector c is perpendicular to the phase surface while the group velocity vector v is parallel to the direction of the beam of seismic energy.

Figure 4: Surface wave anisotropy.

$$\rho V_{SV}^2 = F + G_c \cos 2\theta + G_s \sin 2\theta$$

where V_P is the velocity of the (quasi) P wave, V_{SH} the velocity of the horizontally polarized (quasi) shear wave, V_{SV} the velocity of the vertically polarized (quasi) shear wave, θ the azimuth, and $A, D, F, B_{c,s}, C_{c,s}, E_{c,s}, G_{c,s}$ are constants. For a transversely isotropic material we have $B_{c,s} = C_{c,s} = E_{c,s} = G_{c,s} = 0$.

Similar expressions may be obtained for surface waves (Smith and Dahlen, 1973; Montagner and Nataf, 1986):

$$c(\omega, \theta) = c_0(\omega) + c_1(\omega) \cos 2\theta + c_2(\omega) \sin 2\theta + c_3(\omega) \cos 4\theta + c_4(\omega) \sin 4\theta$$

Since Love waves mainly involve the SH component of movement, the azimuthal anisotropy of Love waves is dominated by the 4θ-terms. On the other hand, Rayleigh waves mainly involve the SV component, and therefore the 2θ-terms dominate the azimuthal dependence of Rayleigh waves.

Seismogical observations of anisotropy

As can be inferred from the above, there are two ways of detecting anisotropy:
(1) by detecting velocity variations as a function of direction,
(2) by detecting differences in velocity as a function of polarization.
A very brief overview of observations is listed below:

1. Azimuthal anisotropy of compressional waves. The primary data in this case are travel time anomalies observed by controlled-source experiments using refracted (P_n) waves. The fast direction in oceanic lithosphere coincides with the (paleo)spreading direction.

2. Azimuthal anisotropy of surface waves. Rayleigh waves have significant azimuthal anisotropy. The direction of the fast Rayleigh waves (with a period of 200 s) does not always agree with the direction of plate motion, but shorter period Rayleigh waves seem to have the fast direction nearly parallel to the paleospreading direction.

3. Polarization anisotropy of surface waves or the so called 'Love-Rayleigh discrepancy'. In some studies phase velocity measurements of both Rayleigh and Love waves for a region cannot be explained by a smoothly varying isotropic model. Most of the oceanic upper mantle shows $V_{SH} > V_{SV}$ anisotropy, and transverse isotropy is usually asumed to describe the velocity

structure. However, more detailed studies show that the polarization anisotropy depends on the depth and age of the oceanic lithosphere.

4. Shear wave splitting. The most decisive observation of anisotropy is shear-wave splitting, and a large number of publications has recently appeared on splitting of SKS phases.

5. Inner core anisotropy. The main data used to study the inner core are short period PKIKP waves and long period normal mode splitting functions. Both data show cylindrical anisotropy (i.e. hexagonal) with the symmetry axis aligned with the Earth's rotation axis.

Figure 3.6-4: Example of anisotropy in the oceanic lithosphere.

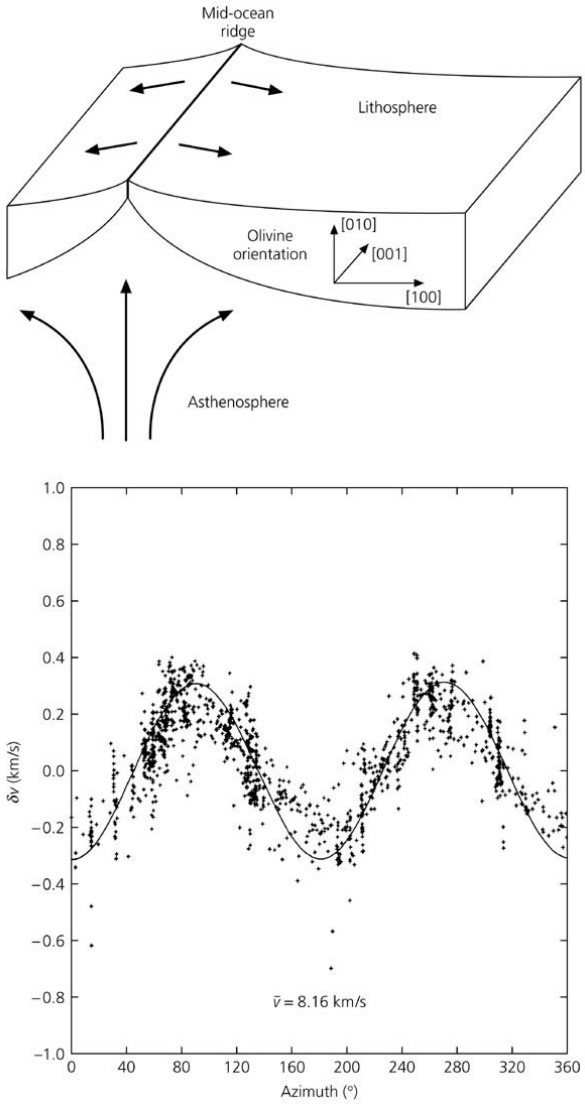

Figure 5: Azimuthal dependence of Pn-wave velocities in the upper most mantle near Hawaii (after Morris et al, 1969).

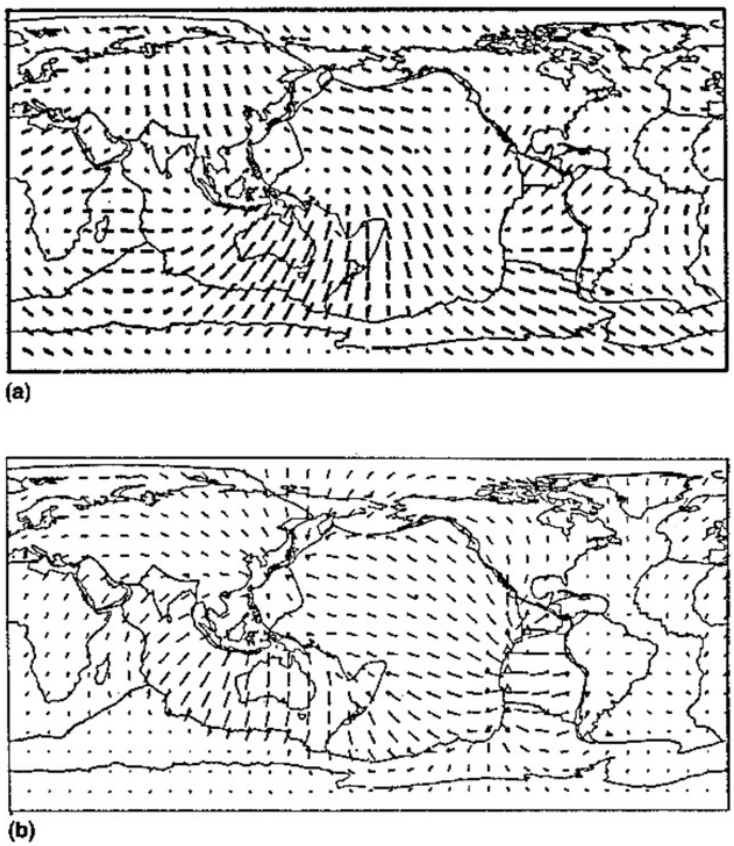

Figure 6: (a) Azimuthal variations of a maximum Rayleigh wave phase velocity at a period of 200 seconds (Tanimoto & Anderson, 1984). (b) Flow lines at 260 km depth in the kinematic model of Hager &)'Connell (1979).

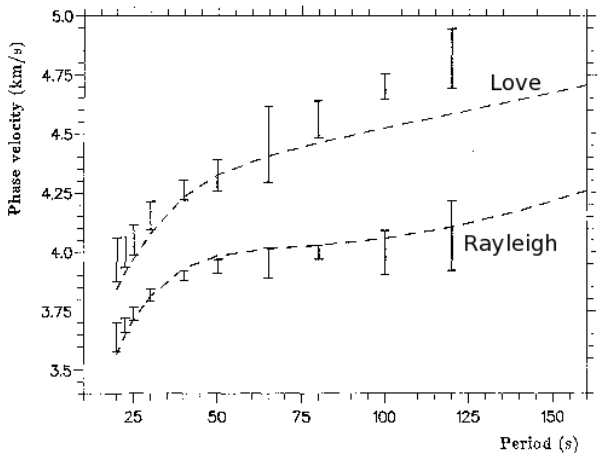

Figure 7: Love and Rayleigh wave measurements for the Iberia peninsula. Dashed lines are isotropic model predictions, which give too low velocities for the Love wave measurements (from Maupin & Cara, 1992).

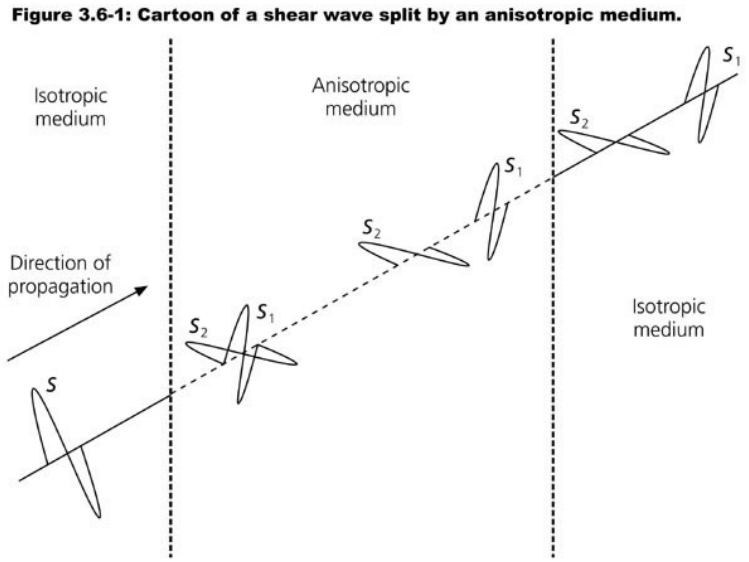

Figure 8: (Sketch showing S-wave splitting due to the transmission through an anisotropic medium. An initial S wave split into two waves S_1 and S_2 when entering the anisotropic medium. Ray tgheory predicts that the two mutually perpendicular polarization vectors can rotate slowly around the ray in a smoothly varying medium.

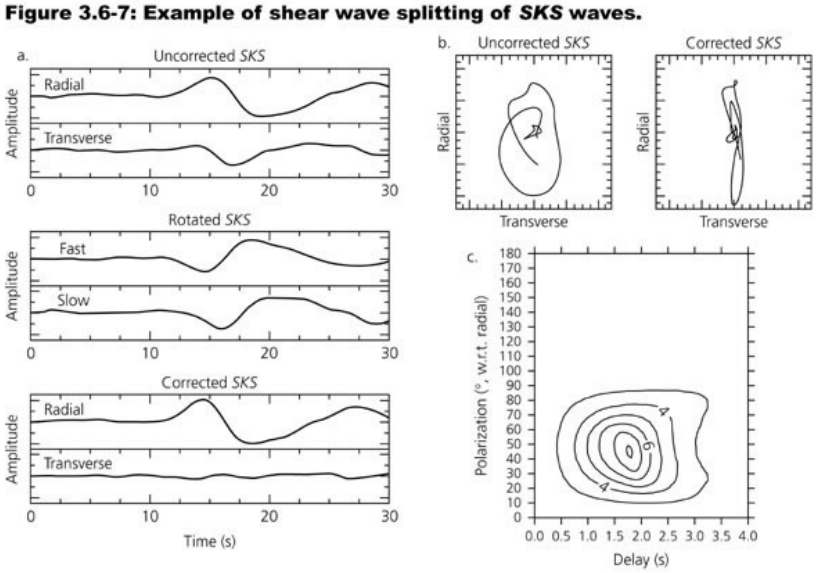

Figure 9: Example of SKS split phases. The transverse component of SKS should not appear if the Earth were representable by a isotropic symmetrically spherical model, and disappares when correcting for anisotropy.

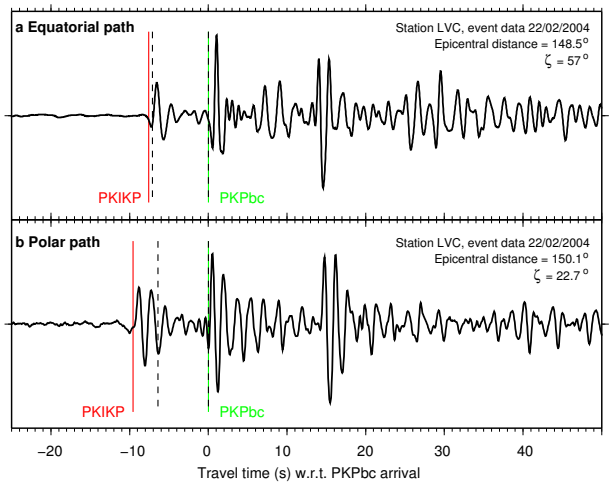

Figure 10: Example of two PKIKP observations (a) for an equatorial path where PKIKP arrives on the predicted time and (b) for a polar path, where PKIKP arrives early because of inner core anisotropy.

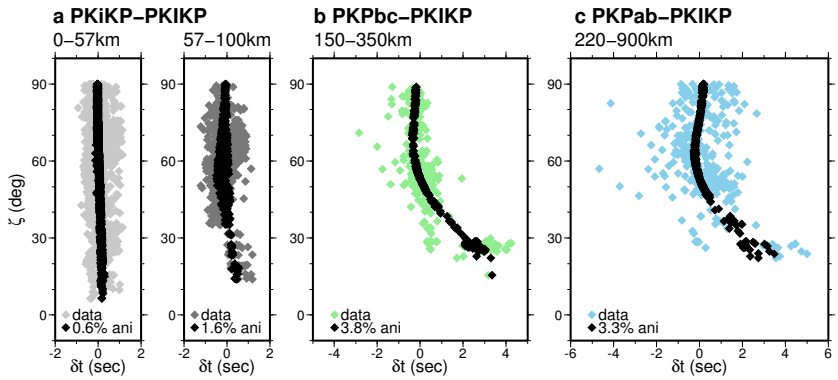

Figure 11: PKIKP data shown as a function of angle ζ with the Earth's rotation axis.

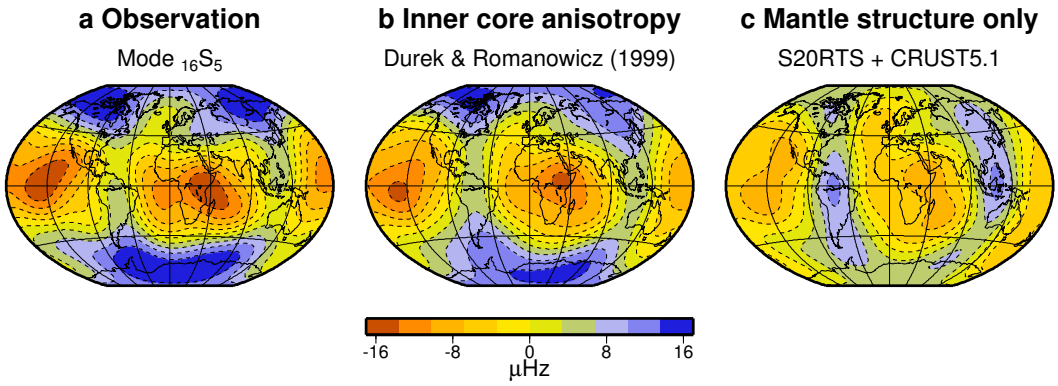

Figure 12: Normal mode splitting function observations of inner core anisotropy. (a) Zonal anisotropy is seen in the data and in (b) Synthetic prediction for inner core anisotropy. Only mantle structure does not match the observed anisotropy.

Causes of anisotropy

There are two causes of anisotropy:

1. Preferred orientation of crystallographic axes of elastically anisotropic minerals such as olivine or orthopyroxene. This type of anisotropy is generally referred to as lattice preferred orientation (LPO). There are two mechanisms to achieve LPO.

   (a) Dislocation glide. Crystallographic axes of each grain rotate because of the constraints of deformation imposed by the surrounding grains. The nature of LPO due to this mechanism depends on the geometrical constraints on the deformation and is related to the flow geometry.

   (b) Grain boundary migration. When there is a large variation in the free energies of the grains and when the grain boundaties are mobile, grains with low free energy will grow at the expense of high free energy grains. Stress controlled seismic anisotropy may thus be formed.

2. Anisotropic shape distribution of isotropic materials, such as laminated structure or fluid filled cracks. The shape of melt pockets is related to the stress distribution. It is expected that in suboceanic lithosphere, where the flow is presumably simple shear in a horizontal plane, the melt-filled cracks will be inclined at 45 degrees with respect to the horizontal plane.

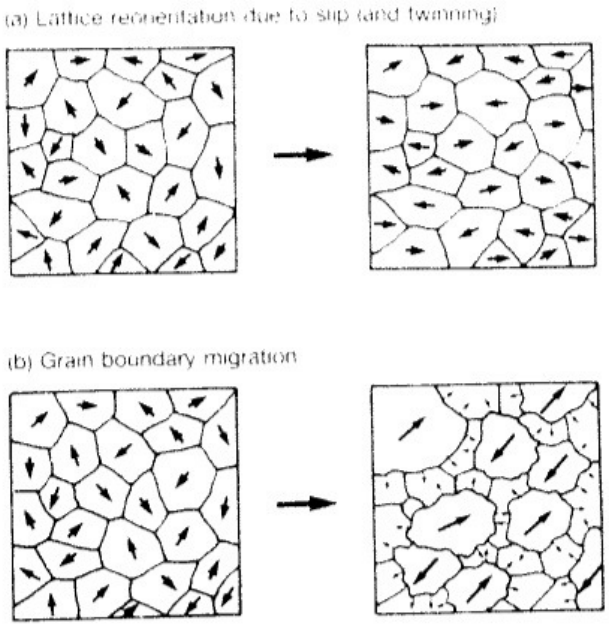

Figure 13: Two mechanisms to get lattice preferred orientation (LPO), (a) dislocation glide and (b) grain boundary migration.